Supporting Information

Ultrafast Plasmonic Hot-Hole Transfer Mediated Efficient Charge Separation in $Cu_{2-x}S$/CdZnS Heterostructure

*Manvi Sachdeva[¥], Nitika Kharbanda[¥], Himanshu Bhatt[ξ], Kaliyamoorthy Justice Babu[¥], and Hirendra N. Ghosh[ξ, *]*

[¥]*Institute of Nano Science and Technology, Knowledge City, Sector 81, SAS Nagar, Punjab-140306, India.*

[ξ] *School of Chemical Sciences, National Institute of Science Education and Research (NISER), Bhubaneswar, Odisha 752050, India.*

[*] *Email:* hnghosh@niser.ac.in , hnghosh2004@gmail.com

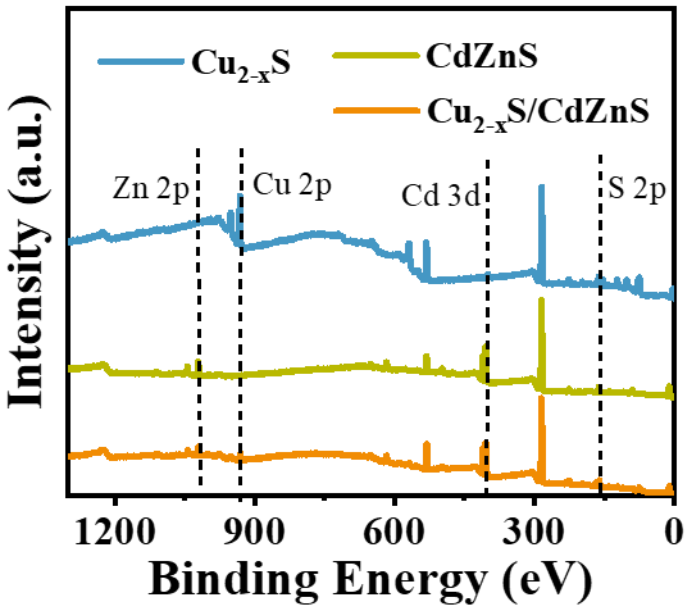

Figure S1. Full survey X-ray photoelectron spectroscopy (XPS) of $Cu_{2-x}S$, CdZnS and $Cu_{2-x}S$/CdZnS.

Table S1. Atomic percentage of $Cu_{2-x}S$, CdZnS and $Cu_{2-x}S$/CdZnS obtained from XPS analysis.

Sample	Copper	Sulphur	Cadmium	Zinc
$Cu_{2-x}S$	54.84	45.16	NA	NA
CdZnS	NA	45.24	27.35	27.4
$Cu_{2-x}S$/CdZnS	31.40	44.74	11.83	12.03

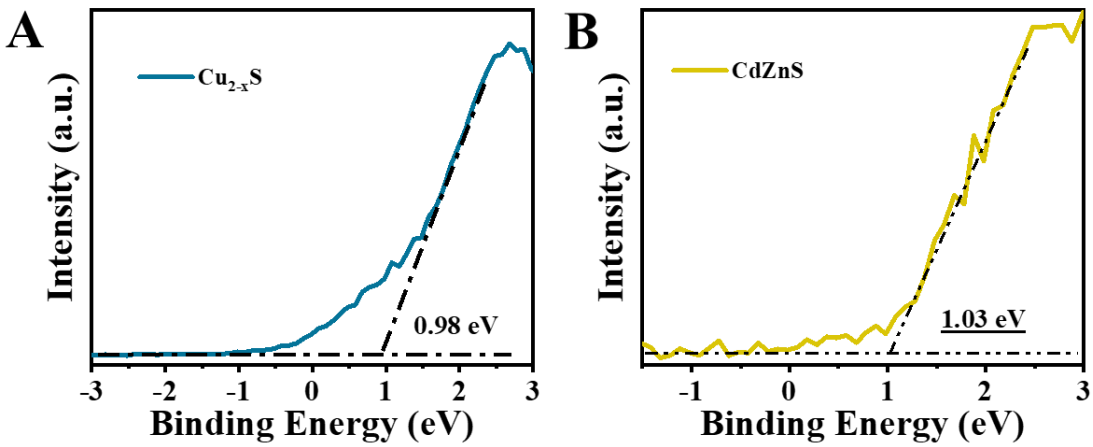

Figure S2. Determination of valence band positions for $Cu_{2-x}S$ and CdZnS from the XPS valence band spectra.

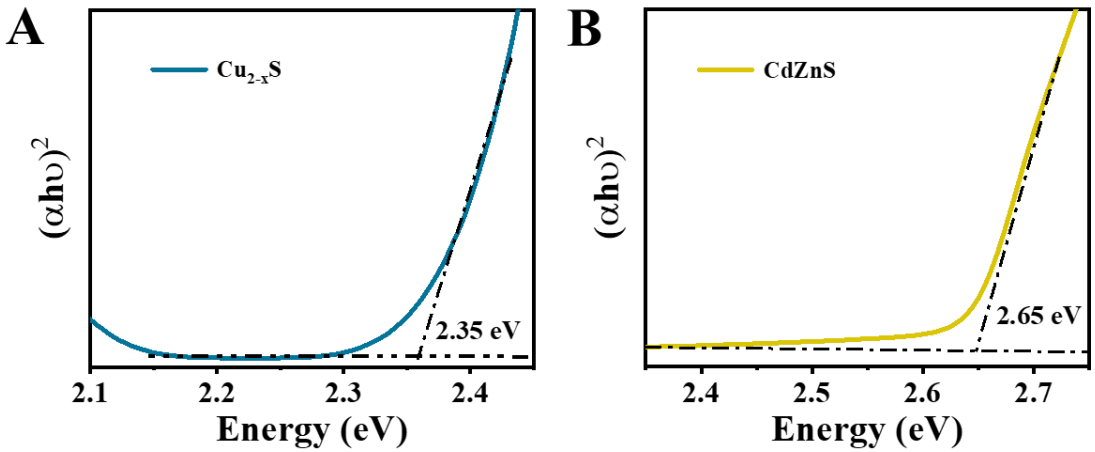

Figure S3. Bang gap calculation for (A) $Cu_{2-x}S$ and (B) CdZnS using tauc's plot method.

Table S2. Atomic percentage of $Cu_{2-x}S$, $Cu_{2-x}S$/CdZnS obtained from EDS.

Sample	Copper	Sulphur	Cadmium	Zinc
$Cu_{2-x}S$	54.73	45.27	NA	NA
$Cu_{2-x}S$/CdZnS	35.72	49.67	9.18	5.43

Table S3. Multiexponential fitting time constants for the bleach growth ($\tau_{h\text{-}h}$) and recovery kinetics ($\tau_{h\text{-}ph}$ and $\tau_{ph\text{-}ph}$) of $Cu_{2\text{-}x}S$ and $Cu_{2\text{-}x}S$/CdZnS at 800 nm excitation.

Sample	Pump (nm)	Probe (nm)	$\tau_{h\text{-}h}$ (fs)	$\tau_{h\text{-}ph}$ (ps)	$\tau_{ph\text{-}ph}$ (ps)
$Cu_{2\text{-}x}S$	800	1180	141 ± 6 (+100%)	0.69 ± 0.02 (-71%)	135 ± 7 (-29%)
$Cu_{2\text{-}x}S$/CdZnS	800	1180	IRF (+100%)	0.63 ± 0.01 (-82%)	60 ± 4 (-18%)

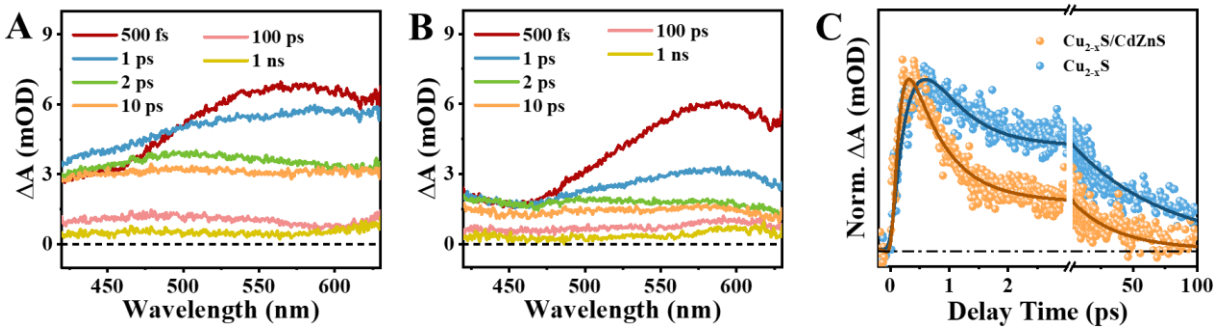

Figure S4. Ultrafast transient absorption (TA) spectra of (A) $Cu_{2\text{-}x}S$, (B) $Cu_{2\text{-}x}S$-CdZnS heterostructure span across visible region (415 nm - 680 nm) at different pump-probe delay times, (C) normalized comparative bleach dynamics between $Cu_{2\text{-}x}S$ and $Cu_{2\text{-}x}S$-CdZnS probed at 500 nm upon 800 nm photoexcitation at fluence of 400 uJcm^{-2}.

Table S4. Multiexponential fitting time constants for $Cu_{2\text{-}x}S$ and $Cu_{2\text{-}x}S$/CdZnS upon 800 nm excitation, probed at 550 nm.

Sample	Pump (nm)	Probe (nm)	growth (fs)	Recovery τ_1 (ps)	Recovery τ_2 (ps)
$Cu_{2\text{-}x}S$	800	550	IRF (+100%)	1.22 ± 0.1 (-61%)	366 ± 10 (-39%)
$Cu_{2\text{-}x}S$/CdZnS	800	550	IRF (+100%)	0.74 ± 0.06 (-84%)	89 ± 6 (-16%)

Table S5. Multiexponential fitting time constants for $Cu_{2\text{-}x}S$ and $Cu_{2\text{-}x}S$/CdZnS upon 800 nm excitation, probed at 500 nm.

Sample	Pump (nm)	Probe (nm)	growth (fs)	Recovery τ_1 (ps)	Recovery τ_2 (ps)
$Cu_{2-x}S$	800	500	0.192 (+100%)	1.03 ± 0.05 (-39%)	117 ± 10 (-61%)
$Cu_{2-x}S$/CdZnS	800	500	IRF (+100%)	0.97 ± 0.05 (-71%)	60± 5 (-29%)

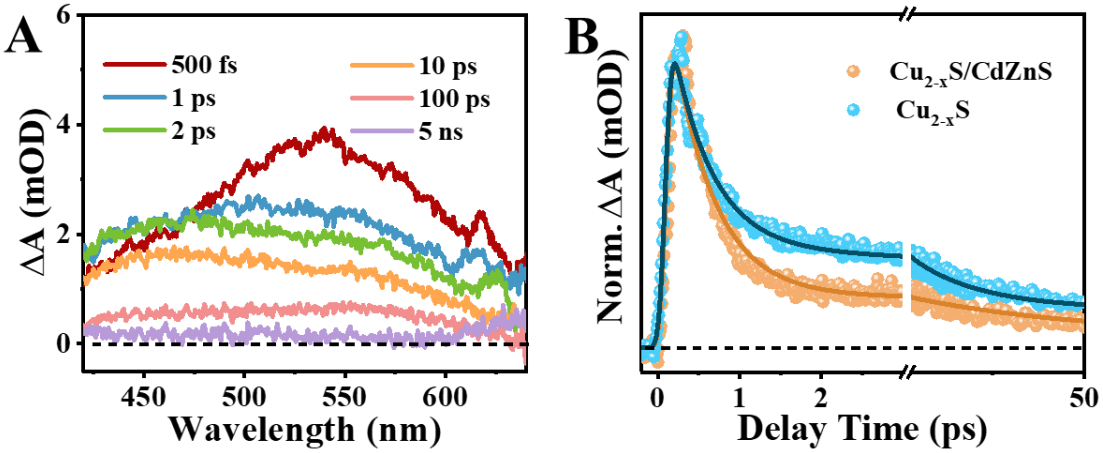

Figure S5. Ultrafast transient absorption (TA) spectra of (A) $Cu_{2-x}S$, span across visible region (415 nm - 680 nm) at different pump-probe delay times, (B) normalized comparative bleach dynamics between $Cu_{2-x}S$ and $Cu_{2-x}S$-CdZnS probed at 550 nm upon 400 nm photoexcitation at fluence of 200 uJcm^{-2}.

Table S6. Multiexponential fitting time constants for the bleach growth ($\tau_{h\text{-}h}$) and recovery kinetics ($\tau_{h\text{-}ph}$ and $\tau_{ph\text{-}ph}$) of $Cu_{2-x}S$ and $Cu_{2-x}S$/CdZnS at 400 nm excitation.

Sample	Pump (nm)	Probe (nm)	$\tau_{h\text{-}h}$ (fs)	$\tau_{h\text{-}ph}$ (ps)	$\tau_{ph\text{-}ph}$ (ps)
$Cu_{2-x}S$	400	1160	180 ± 6 (+100%)	0.74 ± 0.02 (-65%)	235 ± 7 (-35%)
$Cu_{2-x}S$/CdZnS	400	1160	161± 6 (+100%)	0.68 ± 0.03 (-79%)	40 ± 4 (-21%)

Table S7. Multiexponential fitting time constants for $Cu_{2-x}S$ and $Cu_{2-x}S$/CdZnS upon 800 nm excitation, probed at 550 nm.

Sample	Pump (nm)	Probe (nm)	growth (fs)	Recovery τ_1 (ps)	Recovery τ_2 (ps)
$Cu_{2-x}S$	400	550	IRF (-100%)	0.99 ± 0.05 (-69%)	518 ± 38 (-31%)
$Cu_{2-x}S$/CdZnS	400	550	IRF (-100%)	0.92 ± 0.05 (-81%)	311 ± 10 (-16%)

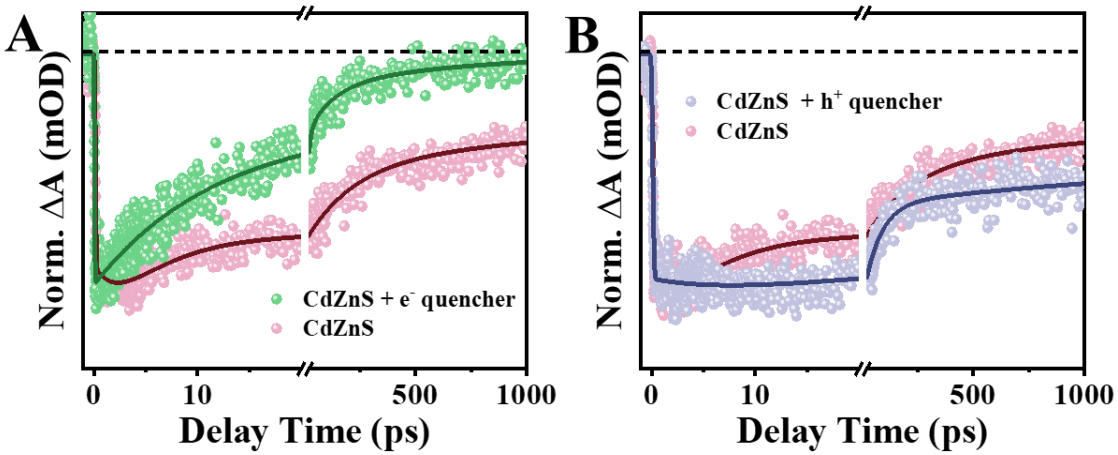

Figure S6. Comparative dynamics between bare CdZnS and in the presence of (A) electron quencher (BQ) and (D) hole scavenger (TEOA) upon 400 nm excitation.

Table S8. Multiexponential fitting time constants for CdZnS, $Cu_{2-x}S$/CdZnS and in presence of electron (BQ) and hole quencher (TEOA) upon 400 nm excitation, probed at 450 nm (band edge bleach).

Sample	Pump (nm)	Probe (nm)	growth (fs)		Recovery τ_1 (ps)	Recovery τ_2 (ps)	Recovery τ_3
CdZnS	400	450	0.33 (-100%)		64 ± 4 (-59%)	744 ± 50 (-25%)	> 1ns (-16%)
$Cu_{2-x}S$/CdZnS	400	450	IRF (-100%)		12.25 ± 0.5 (-82%)	479 ± 40 (-10%)	> 1ns (-8%)
CdZnS + BQ	400	450	IRF (-100%)		19.4 ± 0.9 (-72%)	621 ± 25 (-28%)	___
CdZnS + TEOA	400	450	0.22± 0.01 (-96%)	3.6± 0.8 (-4%)	123 ± 12 (-44%)	> 1ns (-54%)	___